Comparison of different turbulence models in a high pressure fuel jet

Amirhasan Kakaee[1*], Mohammadreza Karami[2]

[1]Associate Professor, School of Automotive Engineering, Iran University of Science and Technology,

[2]MSc, School of Automotive Engineering, Iran University of Science and Technology

ARTICLE INFO	A B S T R A C T
	In this study, modeling of a fuel jet which has been injected by high pressure into a low-pressure tank are investigated. Due to the initial conditions and the geometry of this case and similar cases (like CNG injectors in internal combustion engines (ICE)), the barrel shocks and Mach disk are observed. Hence a turbulence and transient flow will be expected with lots of shocks and waves. According to the increasing usage of this type of injectors in ICE, more studies should be conducted to find the most accurate and beneficial models for modeling this phenomenon. In order to find an accurate and beneficial turbulence model ,in this study, three Reynolds-averaged Navier–Stokes (RANS) turbulence models (SST k-ω, RNG and standard k−ε) and large eddy simulation (LES) turbulence model were compared by the fuel jet characteristics in three regions (outlet of the nozzle, at Mach disk and at the downstream of the flow). Although the LES model needs more time for each test, the results are more reliable and accurate. On the other hand, RANS turbulence models have lots of errors (more than 10 percent) especially for predicting the characteristics of fuel jet at Mach disk.

1. Introduction

The growth of technology and the increase in computing power have made numerical solutions more powerful. Therefore, different models have proposed with more precise results. on the other hand, according to the need of a fast result and a fast model in some cases, computational costs is more important than the margin of error in the final answers from simpler methods[1].

The role of turbulence models is inevitable in computational fluid dynamic (CFD) problems. The most common turbulence models are RANS and LES which are used widely in the numerical approach.

According to what has been said and focusing on the importance of most appropriate turbulence model, comparison of RANS and LES turbulence model have been discussed by many papers in different flow structures like the flow around the bluff bodies which had been discussed by Rodi[2].

According to Banerjee's work[3], to study in-cylinder flows by using LES, one of the expectations is more flow structures are visible than using RANS turbulence models. The main reason for more accuracy in this prediction method is primary and secondary instabilities due

to vertical flow motions in resolved scales in LES turbulence model.

In 2012, Siddhartha Banerjee and Christopher Rutland[4] compared the difference between RANS and LES results for a low-pressure liquid spray induced turbulence by focusing on the grid sensitivity. As a result, they figured out that; with RANS turbulence model the mechanism of gas phase scalar mixing is mainly governed by diffusion in the direction of maximum scalar gridding. While using the LES turbulence model, in addition to the diffusion, an additional mechanism in scalar mixing is observed due to break down of larger fuel-rich pockets into smaller pockets.

On the other hand, the compressed natural gas (CNG), one of the most promising alternative fuels, is widely used in engines due to its rich resource and low price[5]. Although the direct injection technology has been adapted to some gas fuel engine models, the port fuel injection (PFI) is still an important developing direction[6], [7] which is due to fuel jet's characteristics. For instance, a high injection pressure of the stream in the runner of internal combustion engines is turbulence. Therefore, finding an effective turbulence model for investigating the fuel jet and its characteristics in a port fuel injection combustion engine seems to be necessary.

In this study, the comparison between LES turbulence model and three other typical RANS turbulence models including RNG, standard $k - \varepsilon$, and SST k-ω in a high-pressure CNG injector is carried out to suggest the best turbulence model for modeling high-pressure injectors used in internal combustion engines. For this evaluation, the time duration of this simulations and the accuracy of predicting the characteristics of CNG jets injected by high pressure to a low-pressure tank are investigated.

2. Governing equations

The dynamics of fluid flow are governed by equations that describe the conservation of mass, momentum, and energy. The compressible equations for mass transport and momentum transport are given by:

$$\frac{\partial \rho}{\partial t} + \frac{\partial \rho u_i}{\partial x_i} = S \tag{1}$$

And

$$\frac{\partial \rho u_i}{\partial t} + \frac{\partial \rho u_i u_j}{\partial x_j} = -\frac{\partial P}{\partial x_i} + \frac{\partial \sigma_{ij}}{\partial x_j} + \rho g_i + S_i \tag{2}$$

Where the viscous stress tensor will be calculated by:

$$\sigma_{ij} = \mu \left(\frac{\partial u_i}{\partial x_j} + \frac{\partial u_j}{\partial x_i} \right) + (\mu' - \frac{2}{3}\mu) \frac{\partial u_k}{\partial x_k} \delta_{ij} \tag{3}$$

In the above equations, u is velocity, ρ is density, S is the source term, P represents pressure, μ is viscosity, and δ_{ij} stands for the Kronecker delta.

The compressible form of the energy equation is given by:

$$\frac{\partial \rho e}{\partial t} + \frac{\partial u_j \rho e}{\partial x_j} = -P\frac{\partial u_j}{\partial x_j} + \sigma_{ij}\frac{\partial u_i}{\partial x_j} + \frac{\partial}{\partial x_j}\left(K\frac{\partial T}{\partial x_j}\right) +$$
$$\frac{\partial}{\partial x_j}\left(\rho D \sum_m h_m \frac{\partial Y_m}{\partial x_j}\right) + S \tag{4}$$

Where ρ is density, Y_m is the mass fraction of species m, D is the mass diffusion coefficient, S is the source term, P is the pressure, e is the specific internal energy, K is the conductivity, h_m is the species enthalpy, σij is the stress tensor, and T is temperature.

2.1. RANS model description

In this paper, three common RANS models are used, these models are SST k-ω, RNG and standard $-\varepsilon$. All of these models use turbulence kinetic energy (TKE) as their first additional equation. For $k - \varepsilon$ models, the second equation is turbulent dissipation (ε) which is the difference between this two turbulence models[8].

$$\frac{\partial \rho \varepsilon}{\partial t} + \frac{\partial(\rho u_i \varepsilon)}{\partial x_i} = \frac{\partial}{\partial x_j}\left(\frac{\mu}{Pr_\varepsilon}\frac{\partial \varepsilon}{\partial x_j}\right) + c_{\varepsilon 3}\rho\varepsilon\frac{\partial u_i}{\partial x_i} +$$
$$\left(c_{\varepsilon 1}\frac{\partial u_i}{\partial x_j}\tau_{ij} - c_{\varepsilon 2}\rho\varepsilon + c_s S_s\right)\frac{\varepsilon}{k} - S + \rho R \tag{5}$$

Where S is the user-supplied source term and S_s is the source term that represents the interactions with discrete phase (spray). Note that these two terms are distinct. The $c_{\varepsilon i}$ terms are model constants that account for compression and expansion. In the above equation, the term R defines the difference between standard and RNG $k - \varepsilon$ models. In standard $k - \varepsilon$ turbulence model, this term equals zero and for RNG model this term could be calculated by equation no.6.

$$R = \frac{c_\mu \eta^3(1 - {}^\eta/\eta_0)}{(1 + \beta\eta^3)}\frac{\varepsilon^2}{k} \tag{6}$$

Where η is:

$$\eta = \frac{k}{\varepsilon} S_{ij} \qquad (7)$$

And S_{ij} is the mean strain rate tensor.

The k-ω shear stress transport (SST) is actually a combination of RANS, standard $k - \varepsilon$, and standard $k - \omega$ turbulence model. like other RANS k-ω models, this model has two additional equation[8]. One for the transport of turbulent kinetic energy (k) and another one for the transport of specific dissipation rate (ω). These two equations are as follows:

$$\frac{\partial \rho k}{\partial t} + \frac{\partial \rho u_j k}{\partial x_j} = P - \beta^* \rho \omega k + \frac{\partial}{\partial x_j}\left[(\mu + \sigma_k \mu_j)\frac{\partial k}{\partial x_j}\right] \quad (8)$$

And

$$\frac{\partial \rho \omega}{\partial t} + \frac{\partial \rho u_j \omega}{\partial x_j} =$$
$$\frac{\alpha}{v_i} P - \beta \rho \omega^2 + \frac{\partial}{\partial x_j}\left[(\mu + \sigma_\omega \mu_i)\frac{\partial \omega}{\partial x_j}\right] 2(1 - F_1)\frac{\rho \sigma_{\omega 2}}{\omega}\frac{\partial k}{\partial x_j}\frac{\partial \omega}{\partial x_j} \qquad (9)$$

P is production term and α, β, β^*, σ, k are this RANS turbulence model's constants.

2.2. LES model description

A key difference between LES and RANS models is how the fields are decomposed for modeling. For a RANS approach, the field is decomposed into an ensemble mean and a fluctuating component. In the LES approach, the field is decomposed into a resolved field and a sub-grid field. There are two classes of LES models: zero-equation and one-equation. For zero-equation models, the solvers do not solve any additional transport equations[9]. For one-equation models, CFD softwares solve an additional transport equation for sub-grid kinetic energy. In this research, the One-Equation Viscosity Model where used. One-equation viscosity model adds a transport equation for the sub-grid kinetic energy as formulated by Yoshizawa and Horiuti [10]. This model uses the sub-grid kinetic energy for modeling the turbulent viscosity. The sub-grid kinetic energy equation is given by:

$$\frac{\partial k}{\partial t} + \overline{u}_i \frac{\partial k}{\partial x_i} = -\tau_{ij}\frac{\partial \overline{u}_i}{\partial x_i} - \varepsilon + \frac{\partial}{\partial x_i}\left[\frac{v_t}{\sigma_k}\frac{\partial k}{\partial x_i}\right] \qquad (10)$$

And the model for the sub-grid stress tensor is:

$$\tau_{ij} = -2v_t \overline{S_{ij}} + \frac{2}{3}k\delta_{ij} \qquad (11)$$

Where the turbulent viscosity, v_t, is :
$$v_t = C_k k^{1/2} \Delta \qquad (12)$$

Also, the sub-grid dissipation is:
$$\varepsilon = \frac{C_\varepsilon k^{3/2}}{\Delta} \qquad (13)$$

In these equations, Δ is the grid filter, which is related to the cell volume. And it's equal to:
$$\Delta = \sqrt[3]{vol} \qquad (14)$$

C_k and C_ε are adjustable constants for tuning this turbulence model for different usages. In this paper, according to the geometry and the characteristics of the flow, this constants are set as below:

$C_k = 0.05$ and $C_\varepsilon = 1$

3. Validation and grid independency

In this section, validation results and grid independency are presented. Numerical modeling of a high-pressure jet injected into a low-pressure tank whit LES turbulence model where validated against experimental data in Vuorinen et al.'s [11][12] study. They used a geometry provided in figure no.1 with the initial values equals to table no.1.
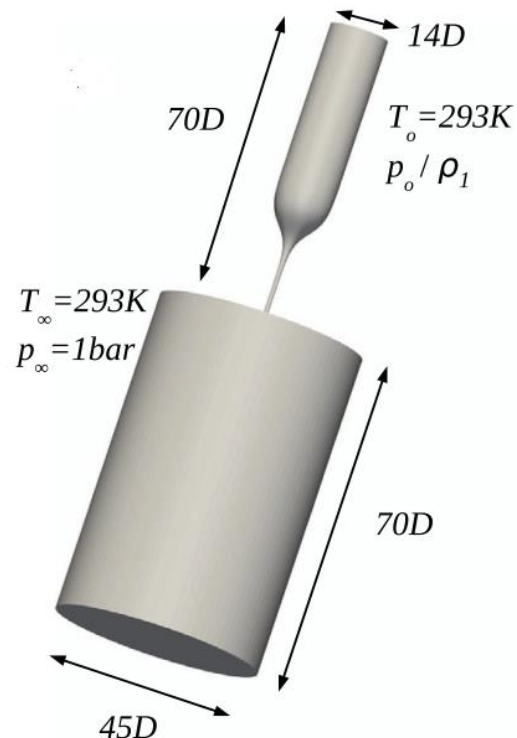

Figure 1: The geometry of Vuorinen et al.'s study

The high-pressure tank is filled with pure CH4 and the low-pressure tank is filled with air. D in the geometry of this study (the diameter of the

Comparison of different turbulence models in a high pressure fuel jet

nozzle) equals to D=0.0014 m and the injection

time duration equals to 0.5 ms.

2: Comparison of different meshing strategy and comparison of fuel jet characteristics from Vuorinen et al.'s paper and different mesh strategies used in this study[12]

	Embedding size of inner cylinder	Embedding size of outer cylinder	Number of active cells	Time of computing (s)	v_{nozzle} (m/s)	ρ_{nozzle} $(\frac{kg}{m^3})$	W_{disk}/D	H_{disk}/D	ρ_{disk} $(\frac{kg}{m^3})$
Vuorinen et al.'s study	Not defined		12000000	Not defined	422.2	1.7	0.14	1.3	0.234
Base grid	0	0	416000	5000	451.6	0.83	No Mach disc were observed		
Embedding no.1	2	1	570000	6000	484.7	1.16	No Mach disc were observed		
Embedding no.2	3	2	900000	14000	463.2	1.35	0.3	1.26	0.381
Embedding no.3	3	3	1800000	60000	436.6	1.55	0.21	1.23	0.349
Embedding no.4	4	3	2500000	147100	423.9	1.62	0.15	1.28	0.232
Embedding no.5	5	4	5100000	320000	422.8	1.62	0.14	1.29	0.235

Table 1: Initial values of Vuorinen et al.'s study

Pressure of high pressure tank	4.5 bar
Pressure of low pressure tank	1 bar
Pressure ratio of injection	4.5
Temp of high pressure tank	293 K
Temp of low pressure tank	293 K
Mass flow	1.1125 g/s

In the Vuorinen et al. research, mesh contains 12 M computational cells, this high number of cells needs lots of computational costs so in this study we used embedding mesh. By this feature, a preset part of the geometry will be modified and the grid scale of this area will be resized by the equation no.15:

$$\Delta l' = \Delta l \times 2^{-n} \tag{15}$$

n is the embedding size which user sets. $\Delta l'$ is the new length scale of grid sell and Δl is the base grid's length.

After choosing a base scale grid (dx= 0.9mm dy= 0.8mm dz= 0.9 mm), two cylinders were set for embedding mesh. Length of this cylinders are 25D and the radiuses of the inner one are D and 3D and for the outer cylinder's radiuses are 3D and 4.5 D.

For mesh independency in this study, the embedding size of these cylinders was changed. Figure 2 shows the base grid and 2 different embedding sizes within a slice in the center of geometry.

In table no.2, these different types of meshing strategies with their number of active cells and the time required for computing this problem are presented. For validation and checking the mesh independency, the characteristics of Vuorinen et al.'s [12] fuel jet were extracted and compared with these different types of meshing strategies.

These characteristics include the velocity and density of CH4 in the outlet of the nozzle, width and height of the Mach disk (shown in figure 3), and the density of CH4 in the Mach disc. The result of this comparison is also presented in table no.2. In this table, the height and width of Mach disc were divided to the diameter of the nozzle to create a dimensionless parameter.
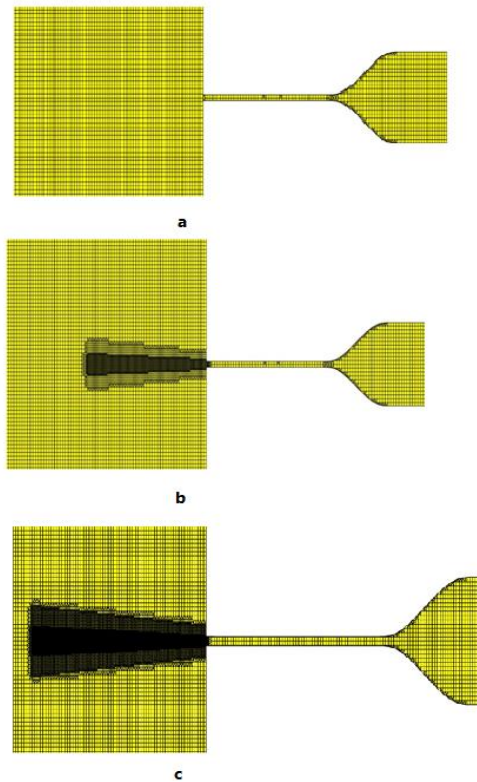
Figure 2: Grid topology in a central slice. a: base grid, b: base grid with embedding by the size of inner cylinder 2 and the outer one 1 . c: base grid with embedding by the size of inner cylinder 5 and the outer one 4


Figure 3: Mach disk and placement of width and height of Mach disc

As it is clear in table 2, the nearest mesh strategy to the results presented by Vuorinen

et al. is embedding no.5. But the difference between embedding no.4 and the results is acceptable. Therefore due to shorter computing time needed for embedding no.4 in comparison with embedding no.5 (according to table 2) and little difference between their results, in this study embedding case 4 were chosen as the grid strategy. It is noteworthy that for validation, if the formula presented by Ashkenaz and Sherman (1966)[13] were used, the acceptable gridding strategy by the error percentage below 10 was gridding with embedding no.3.

In figure 4, the fuel's jet from the outlet of injector's nozzle at the end of the simulation (0.5 ms) conducted by Vuorinen et al. (a) and conducted in the present research (b) are provided. In this research, simulation is carried out by gridding with embedding no.4 which has 2.5 M active cells. As it is clear, the resolution of present study's density graph is lower because of fewer active cells in the domain. However the main characteristics (like the place of barrel shocks and the amount of CH4's density) of fuel jet is in the good agreement with Vuorinen et al.'s study.
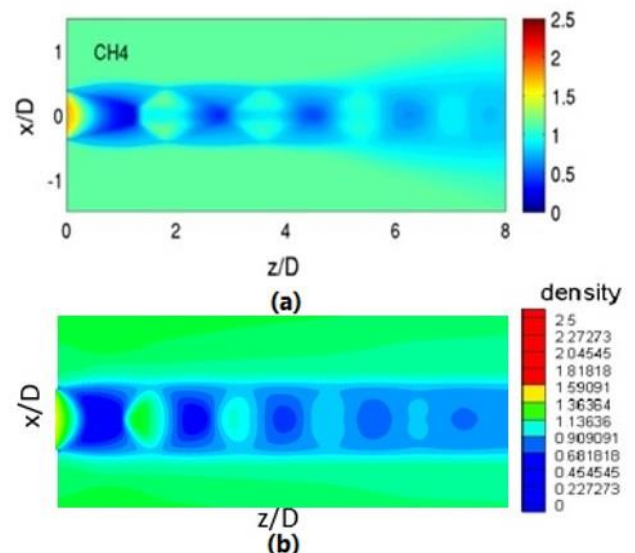
Figure 4 a: fuel's jet at 0.5 ms from Vuorinen et al.'s work -b: fuel's jet at 0.5 ms from this study by chosen gridding strategy

4. Result and discussion

In order to identify the difference between turbulence models for predicting the characteristics of CNG fuel jet injected by high pressure, in this section the results of using noted

turbulence models (including LES-standard $k - \varepsilon$ - RNG $k - \varepsilon$ and SST k-ω) for modeling Vuorinen et al.'s [12] case study are presented and

For more investigation in this study, a segment was chosen normal to the streamline of the fuel jet and at the distance of 25D from the outlet of the nozzle (the topology of this segment is shown in

Table 3: comparison of different turbulence models for predicting fuel jet characteristics and time duration of a test

	Time duration(s)	H_{disk}/D	W_{disk}/D	$v_{nozzle}\left(\frac{m}{s}\right)$	$\rho_{nozzle}(\frac{kg}{m^3})$
LES	147100	1.28	0.15	423.9	1.62
standard $k - \varepsilon$	107800	1.24	0.23	429.3	1.38
RNG $k - \varepsilon$	112400	1.17	0.18	425.7	1.51
SST k-ω	127000	1.10	0.12	428.2	1.57
Vuorinen et al.'s study	-	1.3	0.14	422.2	1.63

compared.

At the end of the simulation, for each turbulence models (at 0.5 ms), the characteristics of fuel jet including velocity ($v_{nozzle}(\frac{m}{s})$) and density of CH4 in the outlet of nozzle ($\rho_{nozzle}(\frac{kg}{m^3})$), width and height of Mach disk (divided to diameter of nozzle) (H_{disk}/D & W_{disk}/D), and the time duration of each test are presented in table 3.

In figure 5, the graph of density for these different turbulence models and Vuorinen et al.'s study at 0.5 ms is presented. As its clear in figure 5 and table 3's data LES turbulence model has the most accurate and precise jet's behavior predictions. For the initial behavior of fuel's jet after LES turbulence model, the SST k-ω turbulence model has acceptable and reliable results due to a small amount of errors for predicting the density of CH4 in the outlet of the nozzle. This region of jet starts from the outlet of the nozzle and continues to the end of barrel shock and facing with Mach disc. For predicting the Mach disc characteristics (including the height and width of it), the most unreliable RANS turbulence model would be standard $k - \varepsilon$ because the error from predicting width of Mach disk is so much (64%). Among two other RANS model, both of them have lots of errors. In RNG $k - \varepsilon$ turbulence model, these errors of calculation for height and width of the disk would be 10 and 27 % and for SST k-ω it would be 15.38 and 20% respectively.
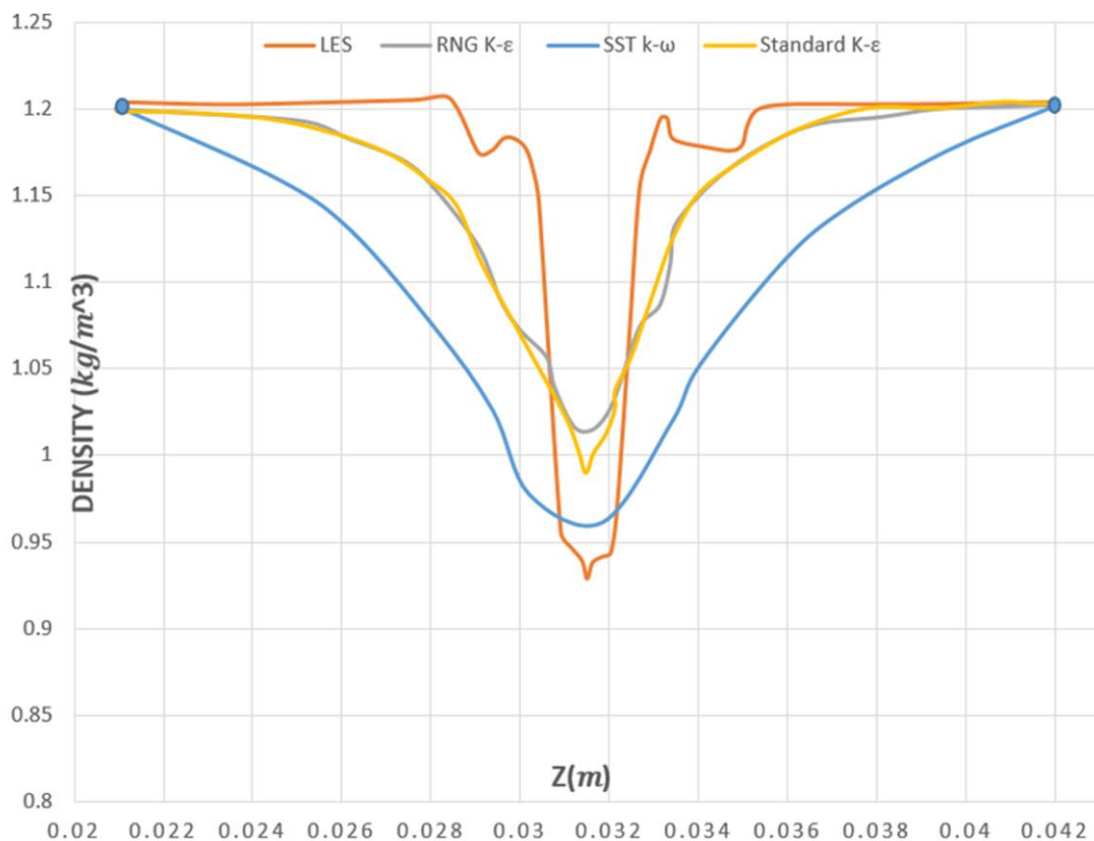
figure 6).

Figure 5 Contour of density at 0.5 ms for **a**: Vuorinen et al.'s study[12] **b**: this study with LES turbulence model – **c**: this study with standard $k - \varepsilon$ turbulence model – **d**: this study with RNG $k - \varepsilon$ turbulence model **- e**: this study with SST k-ω turbulence model

At this segment, the density of fuel (CH4) is measured for investigating the prediction of downstream of the fuel jet's characteristics, for comparing these predictions among different turbulence models, their density-Z graphs are presented in figure 7.
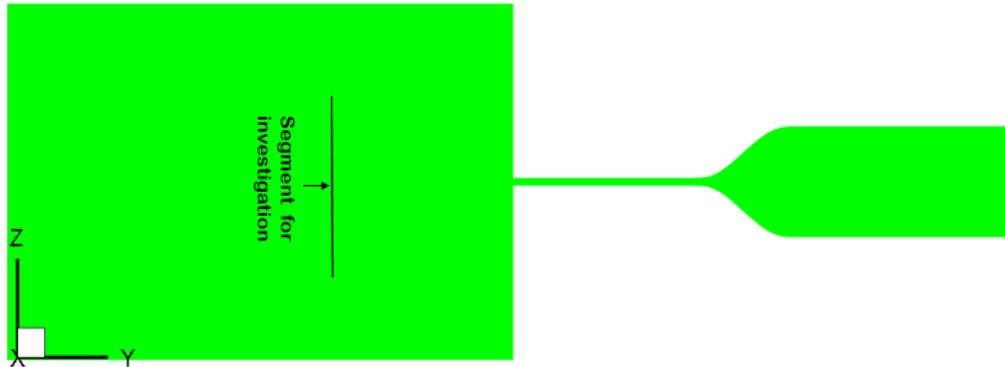
Figure 6 Topology of the segment for investigation of downstream of fuel jets characteristics

Figure 7 Density-Z graph of different turbulence models for downstream of fuel jet's characteristics prediction

As it is revealed in figure 7, the most reliable RANS turbulence model for predicting the downstream characteristics of the fuel jet would be SST k-ω. That is due to little error at the critical point of the graph (Z=0.0315 (m) center line of flow stream) which has the minimum amount of CH4 (3.22% error). Both

standard and RNG $k - \varepsilon$, show similar behaviors at the downstream. In addition, at the critical point of Density-Z graph, RNG $k - \varepsilon$ has the 8% error and Standard $k - \varepsilon$ has 7.3 % error.

5. Conclusions

In this work, a high-pressure fuel jet was injected into a low-pressure tank to compare the results of modeling this phenomenon (high-pressure injection like DI internal combustion engines) by using different turbulence models including three common RANS turbulence models and LES turbulence model. Validation and mesh independency were performed for proving the accuracy of the methodology used for solving these problems. For comparing these turbulence models among time duration of each test, fuel jet's characteristics were extracted in three segments (including the outlet of the nozzle, at Mach disk, and at downstream) and compared.

From this study following observation regarding comparing the data among these segments were recorded:

- By using embedded gridding at this study, the results by using 2.5 M active cells were in a good agreement with concluded results in a simple gridding methodology by 12M actives cells.
- Although LES turbulence modeling time duration for each test is much more than RANS turbulence models, its results are much more precise and reliable (less than 3% of errors in each step.)
- For the initial region of flow and therefore for flows which do not face with barrel shocks and Mach disk, both RNG $k - \varepsilon$ and SST k-ω has acceptable results and can be used for modeling.
- For predicting the characteristics of Mach disk, all of these RANS models were unacceptable due to their high amount of errors (SST k-ω had the minimum amounts of 15.38 and 20% error for calculating the height and width of Mach disk respectively.)
- At the downstream of fuel jet, the most precise turbulence model after LES would be SST k-ω. This is due to its little error at predicting the density of preset segment by comparing it to the results concluded

by using LES turbulence model (3.2% error).

References

[1] E. saadati and M. Zeinolabedini, *basic and advanced simulation principles of computational fluid dynamics with CFX and FLUENT*. 1394.

[2] W. Rodi, "Large-Eddy Simulation and Statistical Turbulence Models: Complementary Approaches," *New Tools Turbul. Model.*, 1997.

[3] S. Banerjee, "Study of Low Temperature Combustion Using Large Eddy Simulations," 2011.

[4] S. Banerjee and C. Rutland, "On LES grid criteria for spray induced turbulence," 2012.

[5] Y. G.-M.- Energy and undefined 2011, "Testing for unit roots, causality, cointegration, and efficiency: The case of the northwest US natural gas market," *Elsevier*.

[6] R. Bircann, Y. Kazour, K. Dauer, M. Fujita, and A. Wells, "Cold Performance Challenges With CNG PFI Injectors," 2013.

[7] M. Soberanis, A. F.-I. journal of hydrogen energy, and undefined 2010, "A review on the technical adaptations for internal combustion engines to operate with gas/hydrogen mixtures," *Elsevier*.

[8] Z. HAN and R. D. REITZ, "Turbulence Modeling of Internal Combustion Engines Using RNG κ-ε Models," *Combust. Sci. Technol.*, vol. 106, no. 4–6, pp. 267–295, Jan. 1995.

[9] C. CFD, *CONVERGE-2.3- MANUAL.* .

[10] A. Yoshizawa and K. Horiuti, "A Statistically-Derived Subgrid-Scale Kinetic Energy Model for the Large-Eddy Simulation of Turbulent Flows," *J. Phys. Soc. Japan*, vol. 54, no. 8, pp. 2834–2839, Aug. 1985.

[11] V. Vuorinen *et al.*, "Large-eddy simulation of highly underexpanded

transient gas jets," *Phys. Fluids*, vol. 25, no. 1, 2013.

[12]   V. Vuorinen, A. Wehrfritz, C. Duwig, and B. J. Boersma, "Large-eddy simulation on the effect of injection pressure and density on fuel jet mixing in gas engines," *Fuel*, vol. 130, pp. 241–250, Aug. 2014.

[13]   Ashkenaz and Sherman, "Rarefied gas dynamics."